ERDC/CHL CHETN-I-??
MONTH 2021

US Army Corps of Engineers®

The Marsh Transect Model: A Simple One-Dimensional Model for Decade-Scale Coastal Marsh Response to Waves, Sediment Supply, and Sea Level Rise

by Douglas R. Krafft, Richard Styles, Joseph Z. Gailani, Candice D. Piercy, Tyler A. Keys, and Matthew L. Kirwan

PURPOSE: This Coastal and Hydraulics Engineering Technical Note (CHETN) documents, introduces, and describes the processes of the Marsh Transect Model (MTM). The MTM simulates coastal marsh edge erosion, elevation change, and future migration into upland areas where possible under wave impact and sea level rise.

INTRODUCTION: While ecological benefits of coastal marshes have long been recognized, recent studies have captured the benefits of coastal marshes in reducing coastal erosion and preventing flood damages to coastal communities (Narayan et al. 2017; Costanza et al. 2008). While recent coastal marsh losses of the last century have slowed due to the advent of protective legislation, threats to coastal marshes continue as sea level rise, coastal development, and declining sediment supplies in many estuaries are leading to continued degradation of many coastal wetlands (Schuerch et al. 2018). Existing, restored, and created coastal marshes are being considered as part of recent and ongoing coastal storm risk management feasibility studies; inclusion of coastal marshes as well as other types of natural and nature-based features (NNBFs) as part of an array of measures requires reasonable assurance of the longevity and sustainability of NNBFs over the project life.

While numerous models have been proposed to predict how coastal marshes will change under future conditions or in response to management actions, the utility of these models for project development has not been determined. Many coastal marsh models initially focused on the complex accretion processes that affect marsh elevation (Warren Pinnacle Consulting 2016; Morris et al. 2002, 2016), but future extent of coastal wetlands is a function of complex ecogeomorphic feedbacks that control not just marsh elevation and biomass production but also edge erodibility and marsh pond dynamics (Mariotti 2020), requiring a more comprehensive modeling approach. As sea level rise accelerates, the capacity of the marsh to migrate to current uplands is also critical since vertical accretion processes are limited (Mitchell et al. 2017). More recent coastal marsh models have adopted two- and three-dimensional approaches that integrate with hydrodynamic models like Delft-3D and ADCIRC (Alizad et al. 2016; Best et al. 2018; Mariotti 2020; Nunez et al. 2020).

The MTM is a variation of the Bay-Marsh-Forest Transect Carbon Model (BMFTCM) (Kirwan et al. 2016) and simulates wave-induced marsh edge erosion, marsh elevation change due to below-ground mineral and organic material, and migration over decadal timescales. This one-dimensional transect model includes more processes than simplistic representations of marsh elevation but does not require full hydrodynamic model integration to run. Key additions in the MTM include temporally explicit wind or wave forcing inputs, non-uniform forcing time-steps, non-uniform cell sizes, and a wider range of conditions, but changes in bay depth (not related to sea level rise) and organic sediment deposition were removed. The MTM allows users to directly specify time-varying forcing in one of three formats: wind speed, wave height and period, or wave energy flux and shear stress. Model changes improved computational efficiency and applicability to existing and proposed coastal marsh projects. The MTM enables the user to specify a large variety of parameters while continuing to allow for unspecified default values where necessary.

INTENDED USES: Proposed coastal marsh nourishment projects, as well as coastal storm risk management studies that define acceptable levels of storm risk according to coastal marsh persistence, must consider how marshes respond to changes in wave energy, sediment supply, or sea level. Future evolution of beach-dune NNBF systems often relies on relatively simple transect models such as Cross-shore Numerical Model (CSHORE) (Johnson et al. 2012), Storm Induced Beach Change (SBEACH) (Larson and Kraus 1989), and XBeach (Roelvink et al. 2009) that provide a compromise between simple zero-order models and more complex two-dimensional (2D) or three-dimensional models that rely on full hydrodynamic model implementations to run. Development of a similar approach for coastal marsh NNBF systems will allow planners and managers to make informed management decisions without requiring full 2D hydrodynamic models of the estuarine system over decadal time-scales. The MTM provides a semi-empirical approach to predicting future coastal marsh extent at a point in the landscape. This can allow planners and engineers to determine (1) if the selected location is viable for the continued persistence of a coastal marsh, (2) what (if any) structures may be required to maintain the coastal marsh, (3) the capacity of the marsh to reduce erosion and attenuate waves and/or storm surge in the future, and (4) the maintenance requirements to achieve required coastal marsh geometry.

MODELED PROCESSES: The MTM simulates coastal marsh edge erosion, elevation change within the marsh, and migration into upland areas through seven basic processes: marsh edge erosion, sediment suspension, sediment deposition, belowground biomass growth, decomposition, un-vegetated marsh edge cell flooding, and sea level rise (Figure 1). Modeled marsh edge erosion and sediment suspension operate on an independent wave time-step (dt_w). Sediment deposition and belowground biomass growth interact with marsh edge erosion and sediment suspension processes on the overall model time-step (dt). The MTM evaluates sediment deposition and belowground biomass growth concurrently at a shorter marsh time-step (dt_M). Belowground biomass is decomposed, and sea level rises at the overall model time-step (dt). Edge cells without belowground biomass growth are flooded at integer overall model time-step intervals (dt_{fl}). For many examples, users only need to directly specify an overall model time-step (dt). If averaged wind or wave forcing conditions are used, the wave time-step (dt_w) can use the overall model time-step. The model supplies a default for the marsh time-step (dt_M) of 1:500 of the overall model timestep, which is adequate in most cases. The edge cell flooding time-step (dt_{fl}) uses the overall model time-step unless specified. Specifying larger edge cell flooding time-steps can be used to limit or ignore the removal of marsh edge cells deeper than any of the specified plant communities can grow.

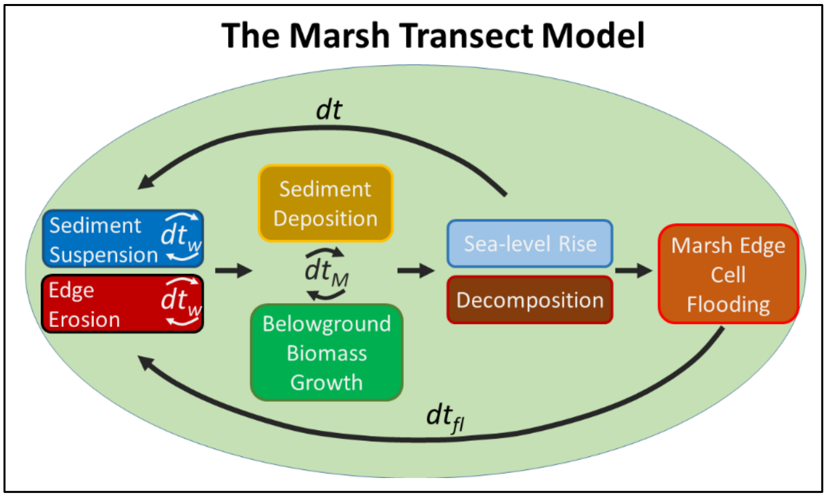

Figure 1. Flow chart of the processes in the MTM and associated time-steps.

Marsh Edge Erosion. The MTM predicts edge erosion distances for each specified wave condition. The edge erosion rate (E) is related to wave energy flux (W) as

$$E = B_e \cdot W \cdot \cos(\theta) \quad (1)$$

where B_e is a marsh edge erodibility coefficient and θ represents an optional wind or wave angle. Users must tune the marsh edge erodibility coefficient with observed marsh edge retreat rates. Previous models (e.g., Kirwan et al. 2016; Mariotti and Fagherazzi 2013; Mariotti and Carr 2014) do not include forcing angle, and the authors did not find previous examples of marsh edge erosion models including forcing angle. The MTM considers user-specified wind or wave angles as relative to the simulated marsh transect with an angle of 0° corresponding to the shore-normal direction. If no forcing angles are specified, the MTM considers the forcing to be entirely normal to the marsh edge, the $cos(\theta)$ term becomes 1, and all of the wave energy flux contributes to marsh edge erosion.

Previous works (e.g., Kirwan et al. 2016; Mariotti and Fagherazzi 2013; and Mariotti and Carr 2014) related marsh edge erosion to both wave energy flux and suspended sediment concentration. The MTM follows the findings of Leonardi et al. (2016) and uses a direct proportionality between marsh edge erosion rate and wave energy flux (Equation 1). Each edge erosion equation requires a specifically tuned marsh edge erodibility coefficient (B_e). As an example, a marsh edge may be subjected to a wave climate represented by a wave height of 0.19 m[1] and a wave period of 1.9 s reaching the marsh edge in 1.5 m of water. Following linear wave theory, that corresponds to a wave power of 37 Watts per meter. If a shoreline erosion rate of 0.5 m/yr has been observed at the site, the appropriate edge erodibility coefficient (B_e) should be selected as $4.29 \cdot 10^{-10}$ m^2/Watt/s.

[1] For a full list of the spelled-out forms of the units of measure used in this document, please refer to US Government Publishing Office Style Manual, 31st ed. (Washington, DC: US Government Publishing Office 2016), 248-52, https://www.govinfo.gov/content/pkg/GPO-STYLEMANUAL-2016/pdf/GPO-STYLEMANUAL-2016.pdf.

Edge erodibility can span a large range of values between different systems and is sensitive to the depth at which wave power is calculated. The MTM also provides an option for users to input wave forcing directly and apply whichever wave transformation model is deemed most appropriate outside of the model. Direct wave forcing input also facilitates the future inclusion of data from forcing due to vessel wake, along with the effects of wave energy-reducing features such as dredge material placements or novel breakwater techniques.

Bay Sediment Suspension. The MTM calculates suspended sediment concentration for the shear stress associated with each forcing condition. The present model iteration follows Mariotti and Carr (2014) and Smith and McLean (1977) and computes the reference suspended sediment concentration over a mudflat as

$$C_r = \rho\lambda\frac{\tau - \tau_{cr}}{\tau_{cr}}\left(1 + \lambda\frac{\tau - \tau_{cr}}{\tau_{cr}}\right) \tag{2}$$

where

- ρ = the bulk sediment density (kg/m^3)
- λ = a non-dimensional sediment erodibility coefficient
- τ = shear stress (Pa)
- τ_{cr} = critical shear stress (Pa).

The suspended sediment concentration entering the marsh uses the sum of C_r and an externally supplied sediment concentration C_o provided as input to the model by the user. The user can also input a time-series of suspended sediment concentration entering the marsh and circumvent sediment suspension calculations.

Marsh Sediment Deposition. The mass of sediment deposited on the marsh within each cell is a function of the suspended sediment concentration and the water depth over each cell throughout the tidal cycle. Sediment accumulation is related to the fraction of the tidal cycle that each cell is submerged. The model follows Kirwan et al. (2016) and expresses the approximation for the mass of deposited sediment as

$$susp\_dep(x) = \sum_{i=1}^{P/dt_d} C(depth_i > 0) \cdot ws \cdot dt_d \cdot dx(depth_i > 0) \cdot \frac{dt}{P} \tag{3}$$

where

- P = the tidal cycle duration (s)
- dt_d = a constant time step (s) over which sediment is deposited (default $P/500$)
- $depth_i$ = the depth (m) relative to the tide level at each point in the marsh
- $C(x)$ = the suspended sediment concentration (kg/m^3) at each point along the transect in the marsh
- $C(depth_i > 0)$ = the suspended sediment concentration (kg/m^3) at each point along the transect in the marsh that is submerged at a specific portion of the tide
- ws = sediment fall velocity (m/s)
- $dx(depth > 0)$ = the transect cell spacing (m) at each cell submerged in a specific tidal section i
- dt = the amount of time (s) simulated at these conditions or the overall time step
- $susp\_dep(x)$ = the mass of sediment deposited (kg) within each cell in a given overall model time-step.

Kirwan et al. (2016) describe this approach for sediment deposition as following previous approaches (e.g., Temmerman et al. 2013; Mudd et al. 2009; Marani et al. 2011; D'Alpaos et al. 2007; Kirwan and Mudd 2012; Fagherazzi et al. 2012). Sediment deposition is calculated for one tidal cycle and scaled by the number of tidal cycles per overall model time-step (*dt*). The MTM converts sediment masses and autochthonous carbon masses to elevation changes simultaneously at each marsh time-step (dt_M). The depth term in Equation 3 is updated to include the sediment deposited and belowground biomass grown in the most recent marsh time-step before checking if a cell is submerged at a particular tidal cycle section. A default value of the sediment deposition time-step is 0.2% of the representative tidal duration or 1.5 min for a typical semi-diurnal tide. Sediment deposits (Equation 3) in submerged cells and belowground biomass grow within each marsh time-step (dt_M). Accretion is scaled by the fraction of the coupling interval with the rest of the model and is converted to a new marsh elevation before the next sediment deposition time-step.

Sediment density after deposition does not presently impact elevation calculations in the MTM, so all sediment is assumed to be mineral, and is described by the constant mineral sediment density that the user is able to specify. The BMFTCM calculates an organic fraction of the sediment suspended in the bay based on the marsh material eroded from the edge, deposited both mineral sediment and allochthonous carbon on the marsh. This feature was removed in the MTM because the BMFTCM did not include compaction, so autochthonous carbon that was eroded from the marsh and reintroduced to the marsh as allochthonous carbon sediment deposition occupied the same volume throughout the remaining simulation. Here, allochthonous carbon refers to carbon in organic sediment suspended in the bay. Autochthonous carbon is used here to refer to belowground biomass that has grown within the marsh and will decompose. Sediment density can often have substantial impacts on marsh elevation, but the processes of sediment compaction and dewatering were omitted, following the BMFTCM. Keeping user input requirements manageable has been an important concern throughout the development of the MTM, and a suitable model for marsh sediment density changes that did not substantially increase the user requirements was not found. Future efforts may be able to include a simple estimate for marsh sediment density changes if a model with suitable input requirements is located. To account for the effects of compaction and dewatering in the present model iteration, users should select a deposited sediment density that matches the long term average for the system.

The MTM applies an exponential decay function to the reference suspended sediment concentration with distance from the marsh edge following Christiansen et al. (2000) and Kirwan et al. (2016). The concentration at each cell is estimated relative to the suspended sediment concentration entering the marsh as

$$C(x) = C_e \cdot e^{-\lambda \cdot x} \tag{4}$$

where

- $C(x)$ = the suspended sediment concentration (kg/m^3) at each cell in the marsh as a function of distance into the marsh x
- C_e = the suspended sediment concentration entering the marsh (kg/m^3)
- Λ = the coefficient for reduction of suspended sediment across the marsh platform (set to 0.0031)
- X = the distance into the marsh (m).

Following the BMFTCM (Kirwan et al. 2016), at each un-vegetated marsh cell, the distance from the marsh edge is reset to incorporate locally entrained sediment, such as in salt marsh pools (Wilson et al. 2014). The BMFTCM and MTM reduce the reference concentration (C_e) by 10% per meter for un-vegetated interior marsh.

The MTM imposes a mass conservation condition on the deposited sediment to prevent mass generation. The maximum possible sediment mass deposited per tidal cycle (*inflow mass*) is computed as

$$zt(x) = \min\left(2 \cdot a, msl + a - marshelevation(x)\right) \tag{5}$$

$$tidal\ prism = \sum\nolimits_{i\ in\ zt>0} zt_i \cdot dx_i \tag{6}$$

$$inflow\ mass = tidal\ prism\ \cdot C_e \tag{7}$$

where

a = the tidal amplitude
msl = the mean sea level
$marshelevation(x)$ = the elevation at each point in the marsh relative to msl
$zt(x)$ = the elevation change in depth at each point in the marsh over the course of a tidal cycle
C_e = the reference suspended sediment concentration at the edge of the marsh (kg/m^3)
tidal prism = the approximation of the volume of water entering the marsh in one tidal cycle (per meter of marsh width)
inflow mass = the sediment mass entering the marsh and available for accretion in a tidal cycle.

The MTM applies accretion by stepping through portions of the tidal cycle and the cells, starting at the marsh edge. If the deposited sediment per tidal cycle (Equation 3) exceeds the inflow mass of sediment per tidal cycle (Equation 7), then the deposition process stops, and the model removes the most recent accretion until mass is conserved.

Tidal signals at marsh sites are often poorly described by a single sine wave. The capability to deposit sediment at elevations more representative of local data is included through an auxiliary function that links consecutive model runs at various tidal ranges for each overall model time-step (*dt*). This results in n_a by n_{dt} individual function calls from the auxiliary function, where n_a is the number of tidal amplitudes chosen and n_{dt} is the number of overall time-steps chosen. Different tidal amplitudes are applied in the user-specified order to maintain repeatable model results. This approach was adopted after attempts to move away from sinusoidal tidal signals within the sediment deposition function were unsuccessful. Stringing consecutive model runs together to represent tidal range variability does increase the computational cost, but simulations evaluate quickly enough that this is not a major concern. Common run times are generally within several minutes.

Marsh Belowground Biomass Growth. Belowground biomass growth is modeled as a parabolic function of depth, with user-defined maximum and minimum depths at which growth can occur (D_{max} and D_{min}) and a coefficient for peak belowground biomass growth rate (B_{max}) following Kirwan and Mudd (2012), Morris et al. (2002), and Kirwan et al. (2016). The model for belowground biomass growth may be expressed in kilograms/cell/year as

$$bgb(x) = \frac{B_{max} \cdot (dm(x) - D_{max})(dm(x) - D_{min})}{0.25(-D_{min} - D_{max}) \cdot (D_{max} - 3 \cdot D_{min})} \cdot dx \tag{8}$$

where $bgb(x)$ is belowground biomass growth rate as a function of distance into the marsh (x) and $dm(x)$ is the marsh surface depth relative to Mean High Water (MHW or $msl + a$) as a function of distance into the marsh. The coefficient for peak belowground biomass annual growth rate (B_{max}) has units of kilograms/square meter/year, so the kilograms/cell/year value is converted to kilograms/cell/second to match the units of the other model components. Belowground biomass growth is evaluated at each marsh time-step (dt_M). Autochthonous carbon masses are converted to elevation changes with sediment masses in each marsh time-step (dt_M). The depth term ($dm(x)$) updates based on the sediment deposited and belowground biomass grown in the previous marsh time-step (dt_M). Some marsh sites contain multiple plant communities, with different belowground biomass growth characteristics, so the model permits the user to specify an arbitrary number of minimum (D_{min}) and maximum (D_{max}) depths as well as either peak growth coefficients (B_{max}) or user-specified growth functions. The specified plant communities can be overlapping or non-overlapping, but competition is omitted, and non-overlapping communities must have non-overlapping boundaries.

Marsh Decomposition. The MTM simulates decomposition through the same relationship as the BMFTCM (Equation 9). This process is described in greater detail in Valentine et al. (citation pending). The mass of autochthonous organic material lost over a year is expressed as

$$decomp(t,x) = organic\ dep\ autoch(t,x) \cdot \left(mki \cdot e^{-\frac{depth(t,x)}{mui}}\right) \tag{9}$$

where

decomp(t,*x*) = the annual rate of decomposition for autochthonous organic material from a specific overall model time-step *t* cohort as a function of distance into the marsh *x*

organic dep autoch(t,*x*) = the mass of autochthonous organic matter remaining in the cohort from a specific overall model time-step *t* as a function of *x*

mki = the annual coefficient of decomposition rate in the marsh

mui = the distance from the marsh surface below which decomposition goes to zero

depth(t,*x*) = the depth beneath the present surface of each mass of autochthonous material deposited at time *t* as a function of *x*.

The mass of decomposed material is corrected for the overall model time-step (dt) and converted to a loss of elevation. Decomposition parameters can be specified once for all plant communities or for each community individually. The decomposition model subtracts elevation within each layer for the sum of the underlying decomposition and stores previous elevations and elevations of sediment cohorts separately.

Flooding of Edge Marsh Cells without Belowground Biomass Growth. After a specified integer number of overall model time-steps (dt_{fl}), cells that are closer to the marsh edge than any cells with belowground biomass growth are flooded (Figure 2), following the BMFTCM. Flooded cell elevations are reduced to the bay depth.

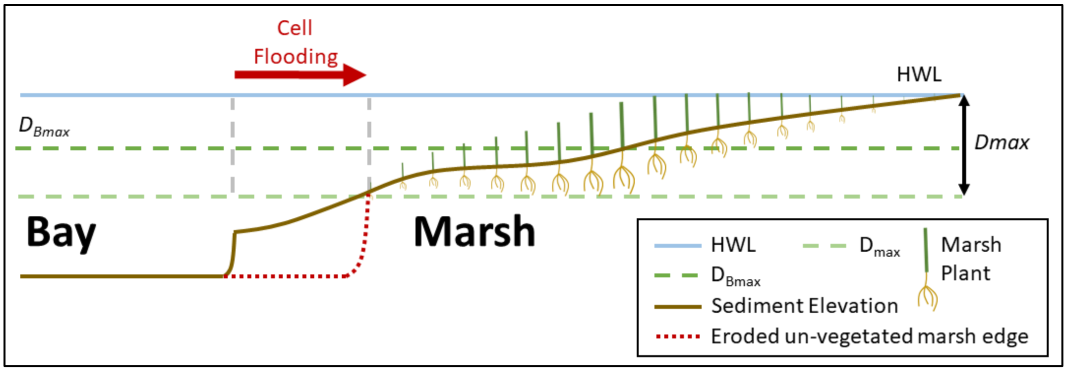

Figure 2. Marsh edge cell flooding of un-vegetated cells based on sediment elevation adjacent to the bay and the maximum depth for modeled plant growth (D_{max}). The depth of peak growth (D_{Bmax}), high water level (*HWL*), and modeled marsh plants are also included for reference.

Marsh Migration and Sea Level Rise. Marsh migration into suitable upland areas and sea level rise have important effects on results from the MTM. Sea level rise alters reference datums throughout the model sub-functions over the course of the simulation. Increases in effective bay depth increase the erosive power of waves and decrease the suspended sediment available for deposition in the marsh. Marsh accretion processes use the high water level (HWL) datum as the sum of the tidal amplitude and the relative sea level rise at that point in the simulation. As sea level rises, the elevation at which belowground biomass can grow likewise increases. Marsh migration into suitable upland areas is modeled by including elevations above the initial high water level, which are included in marsh accretion calculations as they enter the tidal range with relative sea level rise.

INPUT: The MTM is written with the intention of permitting the user to supply available information for each process without limiting the user by excessive data requirements, allowing relatively straightforward model application at a variety of sites. This iteration of the MTM contains a general function that has the capacity to handle a variety of scenarios (e.g., wind or wave forcing, variable stratigraphy, and variable time-steps and grid sizes). The user must specify duration, wind or wave forcing, reference bay concentration, initial marsh width, and bay depth. A sub-function confirms that all required parameters are provided, checks the input structure, and substitutes default values for all fields that the user did not specify.

Wind Input. The MTM is able to force the simulation with wind speed, fetch, and depth using the Young and Verhagen (1996) model for wave height (*Hs*) and period (T_p). Linear wave theory is used to determine shear stress and wave energy flux estimates from wave height and period. The MTM is configured to accept either a single wind speed or a time-series of wind speeds. Applying the Young and Verhagen (1996) model at a shallow depth is substantially different than using the deeper bay depth and transforming the waves into the same shallow depth with more common surf zone models, so the full bay depth is used. The MTM allows users to include wind angle, with the model linearly interpolating between entries in a user-entered table to determine fetch.

Wave Input. The MTM is also able to force the simulation with wave height and period or wave energy flux and shear stress. The model is configured to accept either a time-series of wave heights and periods or a time-series of wave energy flux and shear stresses. If the input includes wave height and period, then these parameters are converted to wave energy fluxes and shear stress by linear wave theory.

Stratigraphy. Stratigraphy is conveyed by a matrix of elevations, a matrix of mineral masses, and a matrix of autochthonous carbon from previous time-steps of deposition and growth in which one axis represents horizontal space and the other axis represents sediment cohort (Figure 5). The user can input information for decomposable organic matter or use an external stratigraphy generation spin-up function adapted from the BMFTCM. This optional function within the MTM generates initial stratigraphy information by the flooding a shallow slope through sea level rise and applying the marsh accretion and decomposition processes (Equation 3, Equation 8, and Equation 9). The MTM is configured to allow a separate relative sea level rise rate for the spin-up. Elevations along a constant slope are flooded by sea level rise until the back edge of the marsh is at the tidal amplitude. A second option allows the user to input a known initial elevation transect, a volumetric fraction of the material that is autochthonous carbon, and a number of initial layers. The second auxiliary function returns evenly spaced layers beneath the specified elevation transect, which decompose according to the specified volumetric fraction of autochthonous carbon.

MARSH TRANSECT MODEL SENSITIVITY: An example case is considered for a 1,000 m marsh of *Spartina alterniflora*, adjacent to a 1.5 m deep and 5,000 m long bay with a reference suspended sediment concentration of 30 mg/L, is forced with a 6 m/s wind, a 1.25 m semi-diurnal tide, and a 1 mm/yr relative sea level rise for 50 yr (Figure 3). The example marsh is also adjacent to 500 m of available upland at a slope of 1:500. The edge erodibility coefficient is tuned to yield 0.5 m/yr. Default values are supplied for all other relevant inputs (details are provided in the Appendix). The MTM is capable of comparing scenarios in which a wide range of parameters is varied simultaneously (e.g., Figure 4), but for simplicity, the sensitivity analysis presented here varies parameters individually. A test matrix of 180 simulations was conducted to emphasize the impact of variations in each variable. As each input is varied, all other inputs are unchanged. In this demonstration bay fetch (*bf*), bay depth (d_b), reference suspended sediment concentration (C_o), edge erodibility (B_e), sediment fall velocity (*ws*), peak belowground biomass growth rate (B_{max}), maximum depth of biomass growth (D_{max}), peak decay rate (*mki*), maximum depth of biomass decay (*mui*), upland slope (*s*), tidal period (*P*), relative sea level rise (*R*), and wind speed (*w*) are varied by a factor of 2. Wave forcing tests are configured to match the waves generated by the 6 m/s wind speed. In wave forcing tests, wave height (H_s), wave period (T_p), wave energy flux (*W*), and wave near-bed shear stress (τ) are varied independently by a factor of 2. As an example, the simulations that vary wave height used the peak period from the baseline condition but did not use a wind speed and calculated wave energy flux and wave near-bed shear stress from the provided input. Initial conditions are generated with the auxiliary spin-up function, and the same initial conditions are used in each test. In this test, parameters are varied within convenient ranges for communicating all results concisely in three subplots (Figure 5). The impact of tidal amplitude is investigated separately (Figure 6).

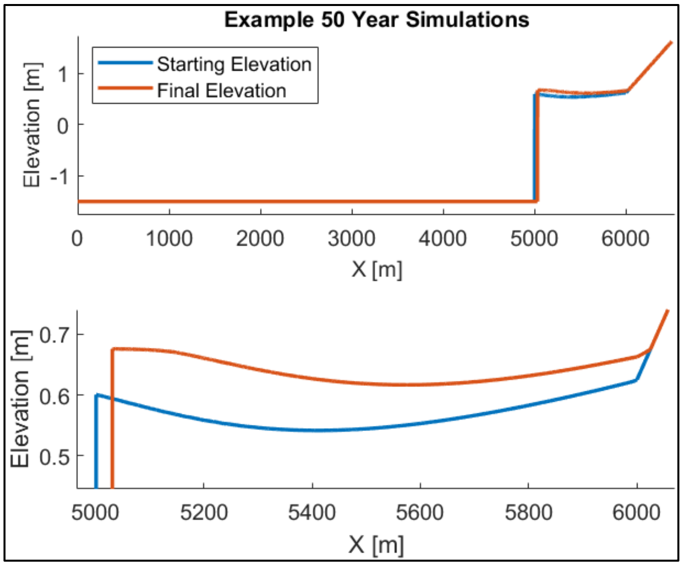

Figure 3. Simulated elevation after 50 yr of forcing. Elevations do not include sea level rise.

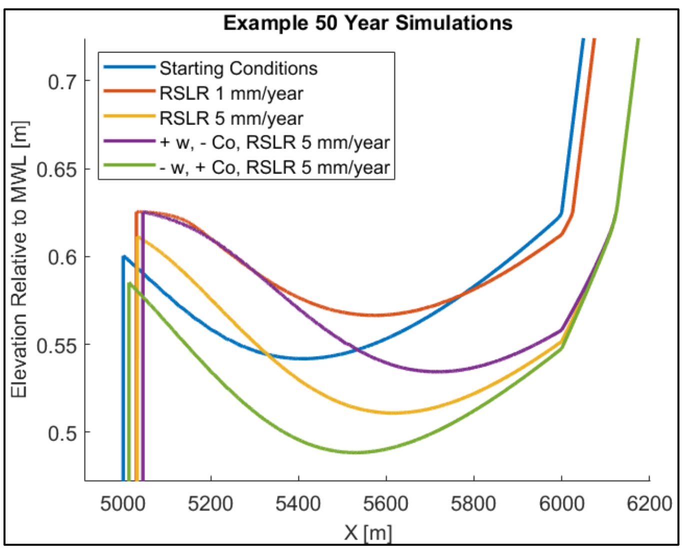

Figure 4. Simulated elevation after 50 yr of forcing. Simulations are compared between cases with accelerated sea level rise; accelerated sea level rise, increased wave energy, and decreased sediment availability; and accelerated sea level rise, decreased wave energy, and increased sediment availability. Elevations relative to Mean Water Level (MWL) reflect sea level rise.

Sensitivity tests are compared by three metrics: (1) average marsh elevation change (Figure 5a), (2) change in marsh width (Figure 5b), and (3) the difference in volumetric fraction of autochthonous organic material in the marsh (Figure 5c). Metrics are presented as the difference from the corresponding metric with the base conditions. All metrics consider the cells above the bay depth but lower than HWL. MHW is the maximum extent of both sediment deposition and belowground biomass growth in this example. Elevation change comparisons account for changes in MWL.

Several variables strongly impact the sediment available to deposit in the marsh in this example. Bay fetch (*bf*) and bed shear stress (τ) have a significant impact on suspended sediment entering the marsh, increasing average marsh elevation and decreasing the organic fraction of the marsh material. Bay depth (*db*) has the opposite effect, with shallower bays suspending more sediment and contributing to more sediment deposition and a smaller fraction of autochthonous carbon. Mudflat critical shear stress (τ_{cr}) also will have an opposite effect to shear stress (τ). Greater values for wind speed (*w*), wave height (*Hs*), and peak period (*Tp*) contribute to more suspended sediment and sediment deposition in the example but also contribute to faster marsh edge erosion. The reference bay suspended sediment concentration (*Co*) contributes less sediment in this case but has a similar effect to bay fetch and bed shear stress.

Sediment fall velocity (w_s) does not appear to have a substantial impact in this simulation. The baseline simulation appears to deposit all sediment contained in the tidal prism, so sediment fall velocities of at least 0.033 mm/s do not cause any differences between the tested simulations. Similarly, longer tidal period (*P*) values distribute the sediment in the tidal prism over a longer timespan resulting in more room for autochthonous organic material, but lower elevations. Faster sediment fall velocities combined with greater suspended sediment concentrations would result in more sediment deposition.

Several growth and decay parameters also influence elevations within the marsh and the fraction of autochthonous organic material. The maximum depth of belowground biomass growth (D_{max}), the coefficient of decomposition (*mki*), and the maximum depth of decomposition (*mui*) correspond with lower marsh elevations and less autochthonous material. Peak belowground biomass growth rate (B_{max}) has the opposite effect and contributes to higher marsh elevations and more autochthonous material.

Changes in marsh width in these examples are a balance between marsh edge erosion and migration into a shallow upland slope. The marsh edge retreats at 0.5 m/yr in the baseline simulation, and the marsh migrates into 0.5 m of previously upland area per year. A more erodible marsh edge (i.e., greater edge erodibility coefficients [*Be*]) or more energetic waves, represented by higher wind speeds (*w*), wave heights (*Hs*), and energy fluxes or longer wave periods (*Tp*), contribute to faster edge erosion. Shallower upland slopes (*s*) and faster relative sea level rise (*R*) contribute to faster marsh migration. Faster relative sea level rises also correspond to more sediment deposition and belowground biomass growth, but in this example these processes add insufficient material to keep pace with rising sea level. The decrease in relative elevation from faster rates of relative sea level rise is countered by migration where a suitable upland environment is available.

Tidal amplitude can have also a large impact on MTM output. Three important distinctions separate the levels of impact: (1) cases where elevation is unknown and plant community growth limits (D_{min} and D_{max}) are tied to MHW, (2) cases where elevation is known and plant community growth limits are tied to MHW, and (3) cases where elevation is known and plant community limits are known separately from tidal amplitude. Results in case 1 change almost linearly with changing tidal amplitude. This results in the same elevations relative to MHW to within several mm, which yields substantial differences relative to MTL. Results in cases 2 and 3 are also sensitive to tidal amplitude (Figure 6). In case 2, higher MHW levels result in more sediment deposition and belowground biomass growth, which can make the difference between keeping pace with and falling behind relative sea level rise, but case 2 elevation increases are smaller than the change in tidal amplitude. In case 3, the updated belowground biomass growth functions decrease elevation gain from autochthonous carbon in the example, resulting in lower elevations in the interior of the marsh than case 1 or case 2 for the same tidal amplitude.

While different combinations of variables will yield different results, preliminary model sensitivity testing indicates that users should carefully select tidal amplitude and wind or wave forcing information and investigate model results under a reasonable range of conditions.

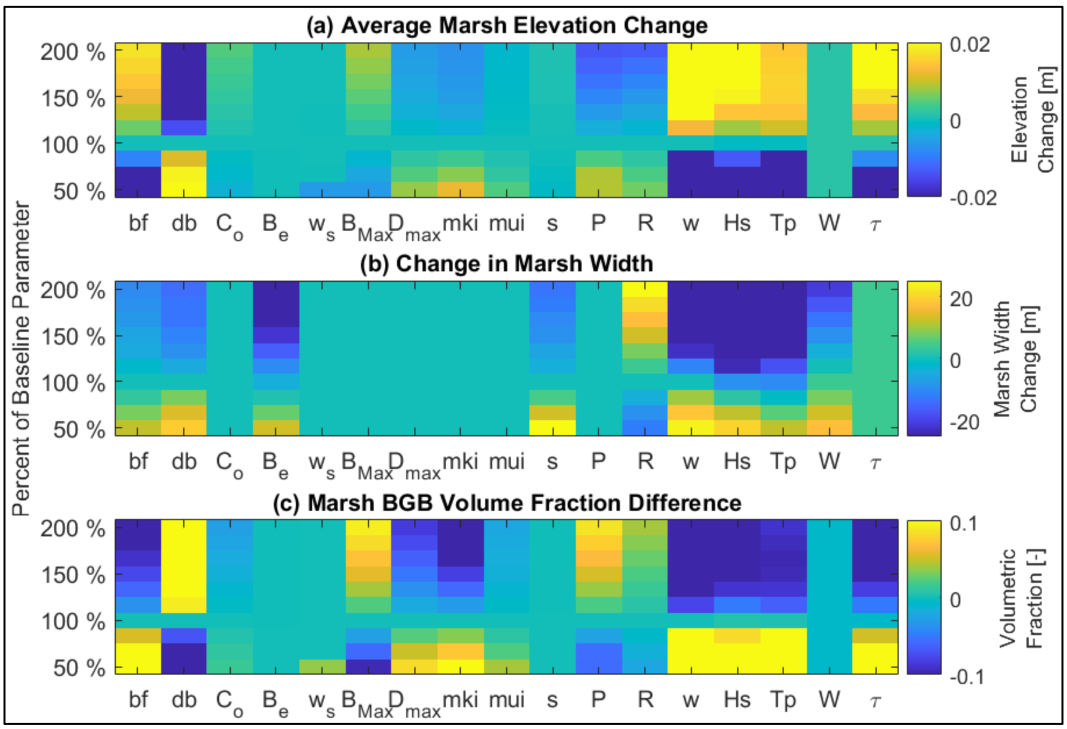

Figure 5. Model sensitivity test in which bay fetch (*bf*), bay depth (*db*), suspended sediment (C_o), edge erodibility (B_e), sediment fall velocity (w_s), peak biomass growth rate (B_{max}), maximum biomass growth depth (D_{max}), coefficient of decomposition (*mki*), maximum decomposition depth (*mui*), upland slope (*s*), tidal period (*P*), relative sea level rise (*R*), wind speed (*w*), wave height (*Hs*), wave period (*Tp*), wave energy flux (*W*), and wave near-bed shear stress (τ) are varied by a factor of 2. Each cell is a unique simulation (a total of 170). Variable names are modified to improve figure clarity. Results are presented relative to model output from baseline parameter simulation.

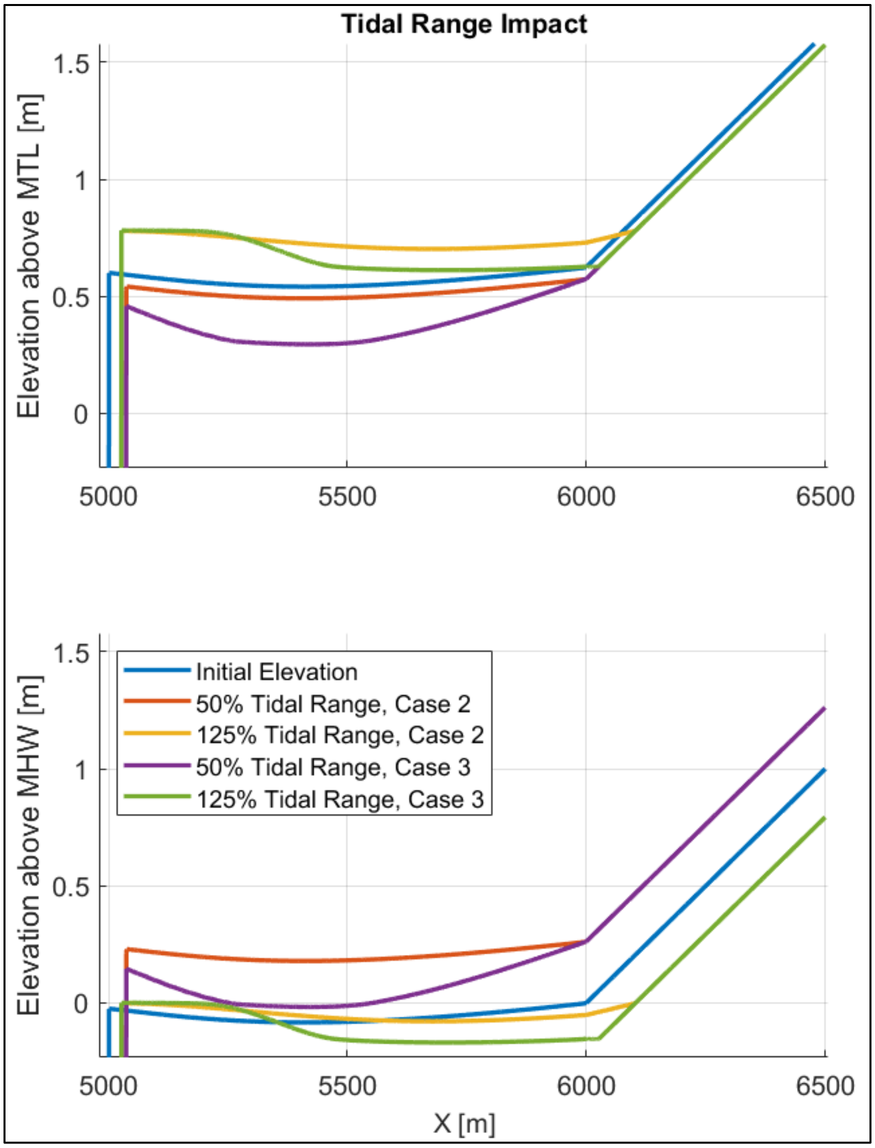

Figure 6. Marsh elevation profiles after 50 yr of forcing at various tidal amplitudes. Case 2 describes belowground biomass (bgb) growth according to the specific tidal amplitude. Case 3 describes bgb growth independently from the specific tidal amplitude.

CONCLUSIONS: This CHETN introduces a semi-empirical model for decadal scale coastal marsh edge erosion, elevation change, and migration driven by changes in wave energy, sediment supply, and sea level rise. The MTM was developed from the Bay-Marsh-Forest Transect Carbon Model (Kirwan et al. 2016) to increase applicability and computational efficiency. The model is configured to use available information without excessive site data collection requirements. While the model does not require the majority of parameters to be specified, users are strongly advised to perform sensitivity analyses before selecting which model results to use in management plans. Simple transect models facilitate decade-scale predictions of coastal marsh persistence and can help planners and managers make informed management decisions where full large-scale and long-term 2-D hydrodynamic models are not feasible. These simple coastal marsh extent predictions can help planners and engineers assess maintenance requirements, future storm surge mitigation, and system longevity and sustainability.

ADDITIONAL INFORMATION: This CHETN was prepared as part of the US Army Corps of Engineers (USACE) Dredging Operations and Environmental Research Program and was written by Douglas R. Krafft (*Douglas.R.Krafft@usace.army.mil*), Richard Styles (*Richard.Styles@usace.army.mil*), and Joseph Z. Gailani (*Joe.Z.Gailani@usace.army.mil*), US Army Engineer Research and Development Center (ERDC) Coastal and Hydraulics Laboratory (CHL); Candice D. Piercy (*Candice.D.Piercy@usace.army.mil*), ERDC Environmental Laboratory; Tyler A. Keys (*Tyler.A.Keys@usace.army.mil*), USACE Sacramento District; and Matthew L. Kirwan (*kirwan@vims.edu*), Virginia Institute of Marine Science, College of William and Mary.

This CHETN should be cited as follows:

Krafft, D. R., R. Styles, J. Z. Gailani, C. D. Piercy, T. A. Keys, and M. L. Kirwan. 2021. The Marsh Transect Model. ERDC/CHL CHETN-I-xx. Vicksburg, MS: US Army Engineer Research and Development Center.

REFERENCES

Alizad, K., S. C. Hagen, J. T. Morris, P. Bacopoulos, M. V. Bilskie, J. F. Weishampel, and S. C. Medeiros. 2016. "A Coupled, Two-Dimensional Hydrodynamic-Marsh Model with Biological Feedback." *Ecological Modelling* 327: 29–43.

D. Roelvink, A. Reniers, J. Ap van Dongeren, Jaap van Thiel de Vries, Jamie Lescinski, and R. McCall. 2010. *XBeach Model Description and Manual*, *Vol. 6*. Deltares, Delft, The Netherlands.

Best, Ü. S. N., M. Van der Wegen, J. Dijkstra, P. W. J. M. Willemsen, B. W. Borsje, and D. J. A. Roelvink. 2018. "Do Salt Marshes Survive Sea Level Rise? Modelling Wave Action, Morphodynamics and Vegetation Dynamics." *Environmental Modelling & Software* 109: 152–166.

Christiansen, T., P. L. Wiberg, and T. G. Milligan. 2000. "Flow and Sediment Transport on a Tidal Salt Marsh Surface." *Estuarine Coastal Shelf Sci.* 50: 315–331.

Costanza, R., O. Perez-Maqueo, M. L. Martinez, P. Sutton, S. J. Anderson, and K. Mulder. 2008. "The Value of Coastal Wetlands for Hurricane Protection." *Ambio* 37(4): 241–248.

D'Alpaos, A., S. Lanzoni, M. Marani, and A. Rinaldo. 2007. "Landscape Evolution in Tidal Embayments: Modeling the Interplay of Erosion Sedimentation and Vegetation Dynamics." *J. Geophys. Res*. 112: F01008.

Fagherazzi, S., et al. 2012. "Numerical Models of Salt Marsh Evolution: Ecological, Geomorphic, and Climatic Factors." *Rev. Geophys.* 50: RG1002.

Johnson, B. D., N. Kobayashi, and M. B. Gravens. 2012. *Cross-Shore Numerical Model CSHORE for Waves, Currents, Sediment Transport and Beach Profile Evolution.* ERDC/CHL TR-12-22. Vicksburg, MS: US Army Engineer Research and Development Center.

Kirwan, M. L., and S. Mudd. 2012. "Response of Salt-Marsh Carbon Accumulation to Climate Change." *Nature* 489: 550–553.

Kirwan, M. L., D. C. Walters, W. G. Reay, and J. A. Carr. 2016. "Sea Level Driven Marsh Expansion in a Coupled Model of Marsh Erosion and Migration." *Geophysical Research Letters* 43(9): 4366–4373.

Larson, M., and N. C. Kraus. 1989. *SBEACH: Numerical Model for Simulating Storm-Induced Beach Change. Report 1. Empirical Foundation and Model Development.* CERC-TR-89-9). Vicksburg, MS: US Army Engineer Research and Development Center.

Leonardi, N., N. K. Ganju, and S. Fagherazzi. 2016. "A Linear Relationship between Wave Power and Erosion Determines Salt-Marsh Resilience to Violent Storms and Hurricanes." *Proceedings of the National Academy of Sciences* 113(1): 64–68.

Marani, M., A. D'Alpaos, S. Lanzoni, L. Carniello, and A. Rinaldo. 2010. "The Importance of being Coupled: Stable States and Catastrophic Shifts in Tidal Biomorphodynamics." *Journal of Geophysical Research: Earth Surface* 115(F4).

Marani, M., A. D'Alpaos, S. Lanzoni, and M. Santalucia. 2011. "Understanding and Predicting Wave Erosion of Marsh Edges." *Geophys. Res. Lett.* 38: L21401. doi:10.1029/2011GL048995.

Mariotti, G. 2020. "Beyond Marsh Drowning: The Many Faces of Marsh Loss (and Gain)." *Advances in Water Resources* 144: 103710.

Mariotti, G., and J. Carr. 2014. "Dual Role of Salt Marsh Retreat: Long-Term Loss and Short-Term Resilience." *Water Resour. Res.* 50: 2963–2974,

Mariotti, G., and S. Fagherazzi. 2010. "A Numerical Model for the Coupled Long-Term Evolution of Salt Marshes and Tidal Flats." *J. Geophys. Res.* 115: F01004.

McKee, K. L., and W. H. Patrick Jr. 1988. "The Relationship of Smooth Cordgrass (*Spartina alterniflora*) to Tidal Datums: A Review." *Estuaries* 11: 143–151.

Mitchell, M., J. Herman, D. M. Bilkovic, and C. Hershner. 2017. "Marsh Persistence under Sea-Level Rise is Controlled by Multiple, Geologically Variable Stressors." *Ecosystem Health and Sustainability* 3:10, 1379888. DOI: 10.1080/20964129.2017.1396009.

Morris, J. T., D. C. Barber, J. C. Callaway, R. Chambers, S. C. Hagen, C. S. Hopkinson, B. J. Johnson, P. Megonigal, S. C. Neubauer, T. Troxler, and C. Wigand . 2016. "Contributions of Organic and Inorganic Matter to Sediment Volume and Accretion in Tidal Wetlands at Steady State." *Earth's Future* 4(4): 110–121.

Morris, J. T., P. V. Sundareshwar, C. T. Nietch, B. Kjerfve, and D. R. Cahoon. 2002. "Responses of Coastal Wetlands to Rising Sea Level." *Ecology* 83(10): 2869–2877.

Mudd, S. M., S. M. Howell, and J. T. Morris. 2009. "Impact of Dynamic Feedbacks between Sedimentation, Sea-Level Rise, and Biomass Production on Near-Surface Marsh Stratigraphy and Carbon Accumulation." *Estuarine Coastal Shelf Sci*. 82(3): 377–389.

Narayan, S., M. W. Beck, P. Wilson, C. J. Thomas, A. Guerrero, C.C. Shepard, B. G. Reguero, G. Franco, C. J. Ingram, and D. Trespalacios. 2017. "The Value of Coastal Wetlands for Flood Damage Reduction in the Northeastern USA." *Scientific Reports* 7, Article number: 9463.

Nunez, K., Y. J. Zhang, J. Herman, W. Reay, and C. Hershner. 2020. "A Multi-Scale Approach for Simulating Tidal Marsh Evolution." *Ocean Dynamics* 1–23.

Roelvink, D., A. Reniers, A. P. Van Dongeren, J. V. T. De Vries, R. McCall, and J. Lescinski. 2009. "Modelling Storm Impacts on Beaches, Dunes and Barrier Islands." *Coastal Engineering* 56(11–12): 1133–1152.

Schuerch, M., T. Spencer, S. Temmerman, M. L. Kirwan, C. Wolff, D. Lincke, and J. Hinkel. 2018. "Future Response of Global Coastal Wetlands to Sea-Level Rise." *Nature* 561(7722): 231–234.

Smith, J. D., and S. R. McLean. 1977. "Spatially Averaged Flow over a Wavy Surface." *J. Geophys. Res.* 82: 1735–1746.

Temmerman, S., P. Meire, T. J. Bouma, P. M. J. Herman, T. Ysebaert, and H. J. De Vriend. 2013. "Ecosystem-Based Coastal Defence in the Face of Global Change." *Nature* 504: 79–83.

Warren Pinnacle Consulting, Inc. 2016. *SLAMM 6.7*, technical documentation. Warren Pinnacle Consulting, Inc. http://warrenpinnacle.com/prof/SLAMM6/SLAMM_6.7_Technical_Documentation.pdf.

Wilson, C. A., Z. J. Hughes, D. M. Fitzgerald, C. S. Hopkinson, V. Valentine, and A. S. Kolker. 2014. "Saltmarsh Pool and Tidal Creek Morphodynamics: Dynamic Equilibrium of Northern Latitude Saltmarshes?" *Geomorphology* 213: 99–115.

Young, I. R., and L. A. Verhagen. 1996. "The Growth of Fetch Limited Waves in Water of Finite Depth. Part 1. Total Energy and Peak Frequency." *Coastal Eng*. 29(1–2): 47–78.

APPENDIX: The model is intended to be applicable across a broad range of conditions, but the test case presented used a particular set of parameters, largely inherited from the work of Kirwan et al. (2016). Table 1 lists the adjustable parameters in the MTM, the values used in the test case, the source.

Table 1. the adjustable parameters in the MTM

Input Parameter	Abbrev.	Value	Source
Edge erodibility coefficient	B_e	$8.75 \cdot 10^{-10}$ m^2/Watt/s	Tuned to match constraints
Marsh Settling Velocity	w_s	$0.05 \cdot 10^{-3}$ m/s	Mudd et al. (2009)
Marsh Settling Velocity (Unused Alternative)	w_s	$0.2 \cdot 10^{-3}$ m/s	Marani (2010)
Tidal Amplitude	*a*	0.625 m	Site-specific input
Maximum depth below HWL for *Spartina Alterniflora* belowground biomass growth	D_{max}	$0.716 \cdot 2 \cdot a - 0.483$ m	McKee and Patrick (1988)
Minimum depth below HWL for *Spartina Alterniflora* belowground biomass growth	D_{min}	0 m	McKee and Patrick (1988)
Coefficient for peak *Spartina Alterniflora* belowground biomass growth rate	B_{Max}	2.5 kg/m^2/yr	Kirwan et al. (2016)
Depth below which decomposition goes to zero in the marsh	*mui*	0.4 m	BMFTCM
Coefficient of decomposition in the marsh	*mki*	0.1	BMFTCM
Mudflat critical shear stress	τ_{cr}	0.1 Pa	BMFTCM